[AMERICAN JOURNAL OF SCIENCE, SCHAIRER VOL. 267-A, 1969, P. 444-462]

# STRUCTURAL EXPLANATION FOR VARIATIONS IN CELL PARAMETERS OF ALKALI FELDSPAR WITH Al/Si ORDERING†

D. B. STEWART* and P. H. RIBBE**

ABSTRACT. Low albite and maximum microcline are assumed to have completely ordered Al/Si distributions, as indicated by resonance spectroscopy and considerations of discrepancies in the linear model relating mean T-O bond length of a tetrahedron to its Al content, and high albite and high sanidine are assumed to be completely disordered. Then relative position on the b-c plot of the point for the cell parameters of an alkali feldspar depends quantitatively on total Al in $T_1O$ and $T_1m$ (triclinic) or in the two $T_1$ (monoclinic) sites. Total Al in the $T_2$ sites, where $T_2O = T_2m$, is obtained by difference. For triclinic feldspars relative position on a $\alpha^*$-$\gamma^*$ plot depends quantitatively on the difference in Al content between the $T_1O$ and $T_1m$ sites. Thus, the distribution of Al over the tetrahedral sites in alkali feldspar of any structural state can now be estimated over a wide temperature range. Specific examples are given for polymorphs of albite, and the details are illustrated of a single ordering process in Na feldspar as a function of temperature involving simultaneous regular migration of Al from $T_2$ sites and the $T_1m$ site into the $T_1O$ site. The ordering process in K feldspar differs conceptually only in initial symmetry restraints; a single process is operative in both alkali feldspar end members.

## INTRODUCTION

Variations in the cell parameters of alkali feldspars have been extensively studied by Wright and Stewart (1968), using natural and synthetic specimens and alkali exchange techniques. They have shown that any (Na, K) feldspar may be chemically identified and characterized as to its relative structural state by the position of its cell parameters on a *b-c* plot (their fig. 2B), particularly when the *b-c* plot is contoured for the *a* axial dimension, which is strongly composition-dependent. For a given composition, the structural state of an alkali feldspar may range between a low albite-maximum microcline equivalent to a high albite-high sanidine equivalent. Crystal structure analyses of eight alkali feldspars (listed in table 1) have shown that the isochemical variations in cell parameters and reciprocal lattice angles, $\alpha^*$ and $\gamma^*$, are related to Al/Si distribution among the non-equivalent tetrahedral (T) sites of the feldspar framework.

The high-temperature feldspars, high albite and high sanidine, are considered to have completely random Al/Si distributions. The low albite-maximum microline equivalents, on the other hand, are highly ordered with most of the Al concentrated into one of the T sites (Al or Si positions), called the $T_1O$ site. However, with presently available techniques the degree of perfection of Al/Si order in feldspars of low structural state cannot be measured quantitatively. The best available functional relationship to estimate the Al content of a T site is a linear model relating the mean T-O bond length of a tetrahedron to its Al content (Smith and Bailey, 1963; Jones, 1968; Ribbe and Gibbs, in press). In constructing such a curve, data are available only for feldspars with the ratio 0.25 to 0.50 Al/Al + Si; therefore, predictions for highly ordered

---

† Publication authorized by the Director, U. S. Geological Survey

* U. S. Geological Survey, Washington, D. C. 20242
** Virginia Polytechnic Institute, Blacksburg, Va. 24061

TABLE 1

Average Al contents of individual tetrahedra for eight alkali feldspar structure analyses, predicted from curve I of Ribbe and Gibbs (in press)*

| | $T_1O$ | $T_1m$ | $T_2O$ | $T_2m$ | Total Al |
|---|---|---|---|---|---|
| Authigenic maximum microcline<br>Finney and Bailey (1964) | 0.85 (0.05) | 0.05 (0.04) | 0.09 (0.04) | 0.02$_5$ (0.04) | 1.01$_5$ |
| Igneous maximum microcline<br>Brown and Bailey (1964) | 0.89 (0.03) | 0.06 (0.02) | 0.03$_5$ (0.02) | 0.04 (0.02) | 1.02$_5$ |
| Intermediate microcline (Spencer U)<br>Bailey and Taylor (1955) | 0.62 (0.04) | 0.26 (0.03) | 0.06 (0.03) | 0.04 (0.03) | 0.98 |
| Adularia (Spencer B)<br>Colville and Ribbe (1968) | 0.38$_5$ (0.02) | 0.38$_5$ (0.02) | 0.11 (0.02) | 0.11 (0.02) | 0.99 |
| Orthoclase (Spencer C)<br>Colville and Ribbe (1968) | 0.33$_5$ (0.02) | 0.33$_5$ (0.02) | 0.15 (0.03) | 0.15 (0.03) | 0.97 |
| Sanidine (heated C)<br>Ribbe (1963) | 0.26 (0.03) | 0.26 (0.03) | 0.23 (0.03) | 0.23 (0.03) | 0.98 |
| Low albite<br>Wainwright and Starkey (1968) | 0.88$_5$ | 0.02$_5$ | 0.06 | 0.05 | 1.02 |
| High albite<br>Ribbe, Megaw, and Taylor (in press) | 0.28 (0.02) | 0.25 (0.02) | 0.22$_5$ (0.02) | 0.25 (0.02) | 1.00$_5$ |

*Estimated standard errors (in parentheses) are calculated from the standard errors in the mean T-O bond lengths using figure 2 of Ribbe and Gibbs (in press) and do not take into account the uncertainties in the linear model assumed for the T-O—Al relationship.

structures whose T sites contain ~0.0 and ~1.0 Al have to be made from long extrapolations of the curve. Many uncertainties associated with the linear model have been discussed at length by Appleman and Clark (1965) and Ribbe and Gibbs (in press) and will not be reiterated here. Suffice it to say that the linear relationship is all that is available, and we have used curve I of Ribbe and Gibbs (in press) in compiling table 1 which shows slightly disordered Al/Si distributions in the three alkali feldspars of low structural state. The differences between perfect Al/Si order and the estimated distributions are statistically meaningful only if the linear model is correct, and since there are arguments from bonding considerations (Brown, Gibbs, and Ribbe, in press) that dispute the linear model, we will assume complete Al/Si order for what are geometrically (= maximum obliquity) the lowest structural states. This assumption is in good agreement with studies of the nuclear magnetic resonance and infrared absorption of highly ordered alkali feldspars by Hafner and Laves, as summarized in Laves and Hafner (1962).

The purpose of this paper is to describe quantitatively the variations of *b* and *c* and $\alpha^*$ and $\gamma^*$ with changes in Al/Si distributions (Stewart and Ribbe, 1967). This will be accomplished by investigating the structures of individual alkali feldspars to determine precisely which bond-length changes (projected onto the *b* and *c* axes) are responsible for changes in *b* and *c*. In any path following bonds through the structure along the *b* direction one $T_1O$, one $T_1m$, two $T_2O$, and two $T_2m$ sites are encountered, whereas along *c*, the sites are $T_1O$, $T_1m$, and either one $T_2O$ or one $T_2m$ site. The projected bond lengths associated with these sites show (as expected) that with ordering Al goes first into the identical and energetically favored $T_1$ sites of monoclinic feldspar from the $T_2$ sites and then into $T_1O$, mainly at the expense of $T_1m$. Since $T_1O$ and $T_1m$ are both always encountered along *b* and *c*, the entry of Al into $T_1m$ has little effect on the cell dimensions. But movements from the $T_2$ sites into $T_1$ sites produce large, quantitatively predictable changes in *b* and *c*. For this reason the total Al in $T_1O$ and $T_1m$ has been taken as the variable against which position on the *b*-*c* plot will be compared. The grouping of $T_1O$ and $T_1m$ together yields a variable that is unaffected by symmetry changes. It will also be shown that for any triclinic feldspar (including plagioclases, which will be dealt with elsewhere), $\alpha^*$ and $\gamma^*$ predict the *difference* in Al content between the $T_1O$ and $T_1M$ sites (see also Ribbe, 1968; J. V. Smith, 1968).

## STRUCTURAL DETAILS OF Al/Si DISTRIBUTION IN ALKALI FELDSPARS

Figures 1A and 1B show projections of part of the structures of sanidine and maximum microcline, respectively, on the plane containing the *b* and *c* axes. Comparison of these projections of the high and low structural states of K feldspar permit us to examine in detail the causes of the changes in axial lengths during the ordering process. Superposition of the projections would show that differences in the positions of the T atoms are very small and that angular relations within and between tetrahedra are the same within 1° or 2° (for specific details see the original structure descriptions). The significant differences between the structures are clearly related to changes in individual T-O distances with Al/Si ordering.

To visualize the collective effect of changes in T-O bond lengths on axial lengths, consider a path through the structure along the *b* direction. One such path (fig. 1) is, omitting the parentheses for clarity, $O_A2$–$T_2O$–$O_BO$–$T_1O$–$O_CO$–$T_2m$–$O_A2$–$T_2O$–$O_Cm$–$T_1m$–$O_Bm$–$T_2m$–$O_A2+$; another is listed in table 2. Since the total of the components of all bonds projected onto an axis equals the axial length, the length is independent

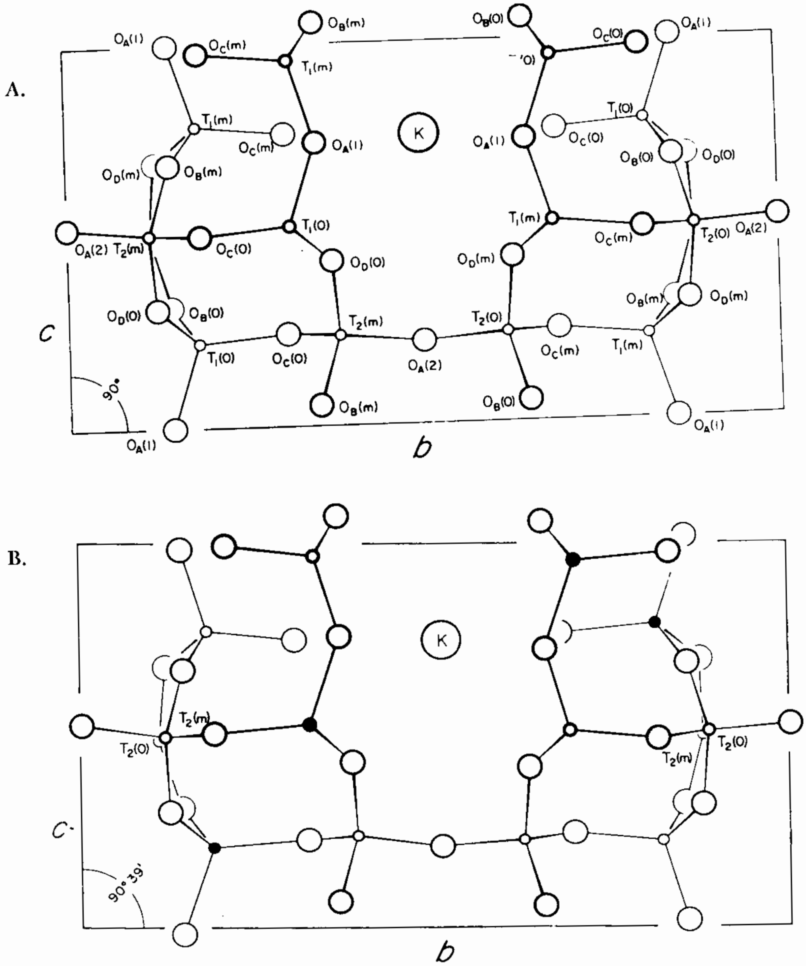

Fig. 1. A portion of the crystal structures of high sanidine (1A) and maximum microcline (1B) projected to scale onto the plane of the *b* and *c* axes. Filled circles in the maximum microcline structure are occupied by aluminum. The labelling of atomic positions is the same in both structures but has been omitted from figure 1B for clarity except for the $T_2$ sites which are superposed in figure 1A.

of path; therefore, the change in axial length with Al/Si ordering is also independent of path. Two examples of paths along *c* are $O_A1$–$T_1O$–$O_BO$–$T_2O$–$O_Dm$–$T_1m$–$O_A1+$ and the one listed in table 2. Notice that all paths along *b* contain sites in the ratio of one $T_1O$, one $T_1m$, two $T_2O$, and two $T_2m$. All paths along *c* also contain one $T_1O$ and one $T_1m$ site, but only one $T_2$ site—either $T_2O$ or $T_2m$. Since the structure analyses of all twelve 7 Å *c*-axis alkali and plagioclase feldspars determined to date have shown the Al content of $T_2O$ and $T_2m$ to be nearly equal, it will probably not matter which path is chosen along *c* when comparisons between ordered and disordered structures are made.

A simplistic approach to the effects of Al/Si ordering on *b* and *c* involves summing the Al encountered along the *b* or *c* path. For both low albite and maximum microcline, the total Al along *b* or *c* is 1.0 (assuming perfect order), because there is only one $T_1O$ site in either path. However, since there are six T sites along *b* and only three along *c*, and all are equally occupied by 0.25 Al (on the average) in the disordered structures, total Al = 1.5 along *b* and 0.75 along *c* for high albite and sanidine. The difference in total Al encountered along these paths going from disordered to ordered states is –0.5 for *b* and +0.25 for *c*. A simple assumption leads to the prediction of the concomitant changes in the *b* and *c* axial lengths.

The curve (Ribbe and Gibbs, in press) that linearly relates Al-content to mean T-O bond length of tetrahedra in feldspars (table 1) extrapolates to T-O = 1.605 Å at Al = 0.00 and to T-O = 1.757 Å at Al = 1.00. A decrease of 0.5 Al along *b* with ordering should result in a decrease in the *b* cell parameter:

$$-0.5\ (1.757\ \text{Å} - 1.605\ \text{Å}) = -0.076\ \text{Å}$$

Similarly an increase of 0.25 Al along *c* ought to cause an increase of 0.038 Å in *c*. Considering differences in alkali atom size and the bonding considerations discussed below which would modify the intercepts, these predictions agree remarkably well with observed values on the *b*-*c* plot (Wright and Stewart, 1968) which shows $\Delta b_{Ab} = 0.087$Å; $\Delta b_{Or} = 0.065$Å; $\Delta c_{Ab} = 0.048$Å; and $\Delta c_{Or} = 0.046$Å.[1]

By a similar argument it can be shown that very little change is expected in the *a* cell edge with ordering. Since all four T sites are encountered in equal numbers in any traverse along *a* (Deer, Howie and Zussman, 1963, fig. 5), then for all structural states of alkali feldspars, total Al along *a* will be 1.00.

It is a moot point whether perfect Al/Si order or partial disorder (as in table 1) is assumed for the feldspars of low structural state. In low albite, for example, total Al is 1.0 for complete order along both *b* and *c*, but using values from table 1 normalized to 1.00 total Al before summing, Al = 0.94 or 0.95 for partial order along *c* and 1.11 Al for partial order along *b*. In either case and for both Na and K feldspar, $\pm\Delta b \approx$

---

[1] This method of predicting cell edge changes also works well for order-disorder transformations in plagioclases. It will be discussed in detail in a forthcoming paper by Ribbe and Stewart.

$\mp 2\Delta c$ (see table 2). Some of the discrepancies of the $\overline{\text{T-O}}$–Al relationship are discussed by Brown, Gibbs, and Ribbe (in press). Briefly, they have shown that bonding considerations—differences in Si-O (→ Si) and Si-O (→ Al) bond lengths (Clark and Papike, 1967), the effects of coordination number of O, the A-O bond lengths and the electron density of the A cation, and the percent $\pi$-bond character of the T-O linkage as a function of T-O-T angle and chemical species at T—are important in determining the final value of an individual T-O bond length, and therefore the mean T-O bond length for a tetrahedron. Taking all these factors into account, it is possible to understand, for instance, why the mean $T_1$m bond length in low albite (as well as in two low oligoclases and an intermediate andesine) is shorter than the $T_2$O and $T_2$m mean bond lengths, even though the Al contents are probably the same. Although precise predictions of Al content are not yet possible, the bonding considerations of Brown, Gibbs, and Ribbe (in press) suggest nearly complete Al/Si order in low alkali feldspars. The analogy of low albite and maximum microcline with the completely ordered reedmergnerite (Appleman and Clark, 1965) and the Al avoidance principle which presumably accounts for the limb of the peristerite solvus at $An_2$ and the nearly complete absence of solid solution in the system Or-An (particularly for the K-rich phases) also suggest complete Al/Si order in alkali feldspars of low structural state. For present purposes, it will be assumed that low albite and maximum microcline are fully ordered.

Turning to table 2 in which the projections, $\Delta_{\text{T-O}}$, of individual T-O bond lengths are listed for short paths along *b* and *c*, the marked similarity between the Na and K feldspar $\Delta_{\text{T-O}}$'s with Al/Si ordering is immediately evident, particularly along *c*. The prominent feature along both paths and for both Na and K feldspars is the substantial increase (0.12-0.14Å) in the sum of the projected $T_1$O-O distances with ordering. This, of course, is expected since Al concentrates in this site. It is of further interest to note that in the comparison of intermediate microcline with maximum microcline (compare table 1 and table 2, column 5), the 0.135Å decrease ($O_D$m–$T_1$m and $T_1$m–$O_C$m) along *b* associated with the $T_1$m site is matched by a 0.139Å increase ($O_D$O–$T_1$O and $T_1$O–$O_C$O) at $T_1$O; along *c* $T_1$O increases by 0.097Å while $T_1$m decreases by 0.071Å. These arise from Al interchange between $T_1$O and $T_1$m. There is a simultaneous net loss of 0.01 to 0.02Å associated with the $T_2$ sites which may be simply second order effects of the interchanges on $T_1$. There is, however, a possibility that a real shift of Al is involved, in which case these $\Delta_{\text{T-O}}$'s may be evidence for a higher degree of Al/Si order in maximum microcline than is predicted by the linear model. *Al* interchange between the $T_1$ sites results in only slight (~ 0.004Å) cell parameter shifts because total Al encountered along *b* and *c* is essentially unchanged; both paths include one $T_1$O and one $T_1$m site. However when Al moves from $T_2$ sites into $T_1$ with increasing order, *b* and *c* change rapidly.

TABLE 2

Changes in individual bond lengths in Angstroms, projected onto the *b* and *c* axes, with ordering in Na and K feldspars*

| Path along *b* | High to low albite | Sanidine to max microcline | Sanidine to Spencer C | Spencer C to intermediate microcline | Intermediate to max microcline |
|---|---|---|---|---|---|
| $O_A2$-$T_2m$ | -0.006 | +0.005 | -0.004 | -0.012 | +0.022 |
| $T_2m$-$O_D0$ | +0.002 | -0.024 | -0.014 | +0.010 | -0.020 |
| $O_D0$-$T_10$ | +0.039 | +0.034 | +0.004 | -0.005 | +0.035 |
| $T_10$-$O_C0$ | +0.097 | +0.099 | +0.011 | -0.017 | +0.104 |
| $O_C0$-$T_2m$ | -0.071 | -0.044 | -0.011 | -0.003 | -0.030 |
| $T_2m$-$O_A2$ | -0.032 | +0.005 | -0.005 | -0.013 | +0.012 |
| $O_A2$-$T_20$ | -0.006 | -0.031 | -0.005 | -0.017 | -0.010 |
| $T_20$-$O_Dm$ | -0.012 | -0.027 | -0.013 | -0.019 | +0.006 |
| $O_Dm$-$T_1m$ | -0.031 | -0.010 | +0.024 | +0.026 | -0.060 |
| $T_1m$-$O_Cm$ | -0.031 | -0.021 | -0.009 | +0.063 | -0.075 |
| $O_Cm$-$T_20$ | -0.007 | -0.021 | -0.010 | -0.030 | +0.020 |
| $T_20$-$O_A2+$ | -0.032 | -0.031 | -0.005 | -0.017 | -0.010 |
| $\Delta b$ | -0.090 | -0.066 | -0.036 | -0.034 | +0.004 |
| Path along *c* | | | | | |
| $O_A1$-$T_10$ | +0.079 | +0.08 | +0.008 | -0.009 | +0.079 |
| $T_10$-$O_D0$ | +0.039 | +0.05 | +0.020 | +0.009 | +0.018 |
| $O_D0$-$T2m$ | -0.024 | -0.02 | -0.017 | -0.025 | +0.022 |
| $T_2m$-$O_Bm$ | -0.021 | -0.05 | -0.017 | +0.014 | -0.044 |
| $O_Bm$-$T_1m$ | +0.026 | +0.02 | +0.014 | -0.005 | +0.015 |
| $T_1m$-$O_A1+$ | -0.049 | -0.04 | +0.009 | +0.035 | -0.086 |
| $\Delta c$ | +0.050 | +0.040 | +0.017 | +0.019 | +0.004 |

*Short paths nearly parallel to the respective axes have been chosen arbitrarily (compare fig. 1).

## STRUCTURAL EXPLANATION FOR POSITION ON THE *b-c* PLOT

The linear relationships shown by plots of the *b* and *c* axial dimensions of all series of alkali-exchanged feldspars were called alkali-exchange paths by (Wright and Stewart 1968). The alkali-exchange paths for potassic and sodic starting materials did not cross and were essentially parallel to the paths for the high sanidine-high albite, and maximum microcline-low albite series, which show complete mutual exchange properties, a consequence of the fact that the *b-c* ratio at a particular alkali composition depends on Al/Si order. Alkali-exchange paths on the *b-c* plot were used as the basis for the qualitative ranking of structural state. We now offer the justification and quantification for that procedure, based largely on structural data for K feldspars.

After careful consideration of the published and unpublished data for the cell edges of feldspars at the corners of the *b-c* plot, we have chosen the following values: low albite, $b = 12.784_4$, $c = 7.157_9$; high albite, $b = 12.871_2$, $c = 7.109_9$; maximum microcline, $b = 12.964_3$,

$c = 7.221_9$; high sanidine, $b = 13.028_9$, $c = 7.176_3$. The lines representing the Na- and K-rich edges of this *b-c* quadrilateral were then divided into ten equal intervals and joined by lines essentially parallel to the low albite-maximum microcline and high albite-high sanidine edges. The low albite-maximum microcline edge was assigned a value of 1.0, and the high albite-high sanidine edge was assigned 0.5. Values of the cell edges as given by the original authors for each of the alkali feldspars whose structure has been determined were plotted, and the proportional distance, $\Delta(bc)$, between the limiting structural states was estimated. In figure 2 these values are plotted against the Al content of $T_1$ sites given in table 1 normalized to 1.00 total Al. A dashed line has been drawn by eye through the data: the relationship is apparently linear[2] but deviates increasingly at more ordered states from the heavy solid line drawn with unit slope. Because errors in determining cell dimensions presumably are random, we interpret the deviation to be another manifestation of the failure of the linear model relating T-O distance and Al content and conclude that the relative position on the *b-c* plot can be used to estimate the Al content of the $T_1$ sites of K feldspars. The relative position on the 060-$\bar{2}$04 plot (Wright, 1968, fig. 3) can also be used similarly to estimate in a simple manner the Al content of $T_1$ sites.

Inspection of a plot of *b* against *c* for various structural states of albite (as in fig. 2B of Wright and Stewart, 1968) shows points in a line similar to that for the structural states of K feldspar. The points on figure 2 obtained by plotting the proportional distance between the line for the maximum microline-low albite series and the line for the high sanidine-high albite series on the *b-c* plot against the Al content of the $T_1$ sites for high and low albite do not differ significantly from the curve for K feldspars, and we assume a linear dependence also occurs for Na feldspars. Our conclusion is to estimate the Al content of the $T_1$ sites of alkali feldspars from the heavy line in figure 2. The Al content of the $T_2$ sites is obtained by difference.

## COMPARISON OF CELL PARAMETERS OF ALKALI-EXCHANGED FELDSPARS

The cell edges of the feldspars at the corners of the *b-c* plot have been plotted against the proportionate distance as used above for K feldspar (fig. 3) and Na feldspar (fig. 4). We also have plotted the values observed by Wright and Stewart (1968, their table 2) for nine feldspars and their alkali-exchanged equivalents in these figures. We do so regardless of the differences in alkali composition because we are comparing against a common variable, the proportionate distance on the *b-c* plot, $\Delta(bc)$.

---

[2] Spencer B, which deviates most from the dashed line, has a high degree of short range order in its pericline- and albite-twin-related domains (Colville and Ribbe, 1968). J. V. Smith (1968) has suggested that short-range (his "local") order accounts for the *b* and *c* cell edges of alkali feldspars. If this can be established, it may be possible to predict from our figures short-range order rather than the long-range order that proceeds from structure analysis.

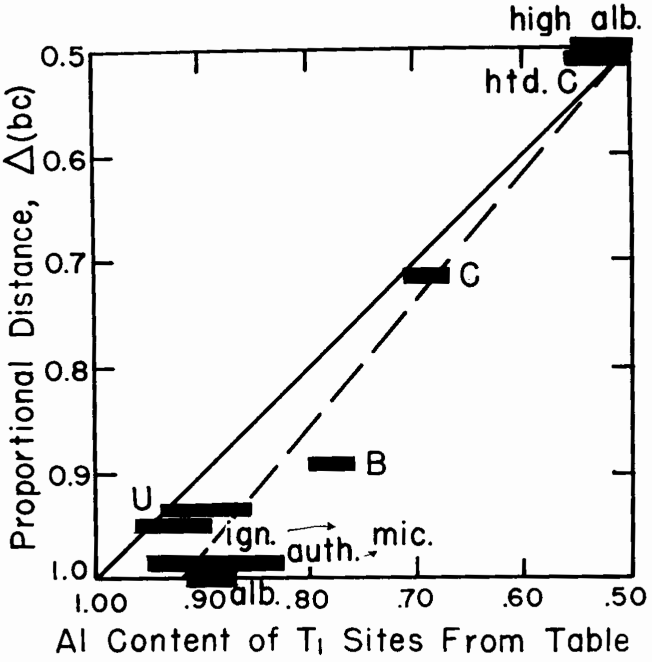

Fig. 2. Al contents of $T_1$ sites from table 1 plotted against relative position on the *b-c* plot for the cell parameters of alkali feldspar. The proportional distance, $\Delta(bc)$, varies only between 0.5 and 1.0, values for the high sanidine-high albite and maximum microcline-low albite series, respectively, chosen so that estimates of the Al content of the $T_1$ sites can be compared directly.

Inspection of the figures reveals that the fit of the cell edges is quite good, providing strong evidence that the Al content of the $T_1$ sites is the same even if the scheme of Al/Si distribution with ordering may not be identical in Na and K feldspars. Because it was not possible to exchange all the K for Na (Wright and Stewart, 1968, p. 69) all the K-rich phases except maximum microcline contained considerable Na (up to 11 atomic percent) in solid solution, and Na has an overwhelming effect on *a* and cell volume. Plots of *a* and cell volume are similar to each other and are not shown principally because of the poor fit of the data for the K-rich phases to the line between the end points. The potassic equivalents of various structural states of albite are all highly potassic, and the data for *a* and volume show only small scatter due to variable composition.

Wright and Stewart (in preparation) will show that the ranges of cell parameters of triclinic and monoclinic K feldspars overlap on figures 3 and 4. We noted above, in the discussion of table 2, that the arrangement of Al between $T_1O$ and $T_1m$ does not affect the estimate of total Al in $T_1$ from the *b-c* plot. On such a plot monoclinic feldspars with balanced Al distributions ($T_1O = T_1m$) cannot be distinguished from intermediate microclines with unbalanced distributions but with the

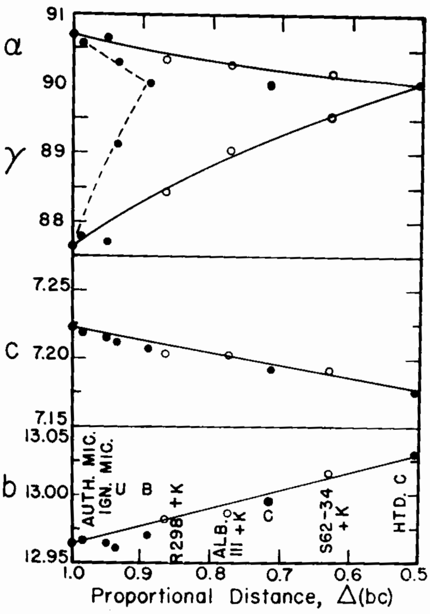

Fig. 3

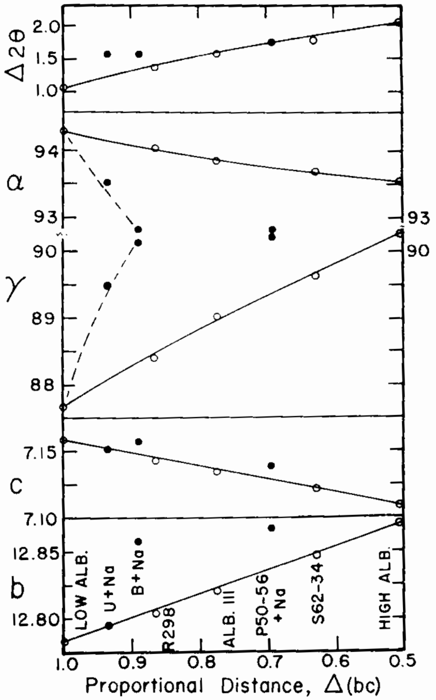

Fig. 4

Fig. 3. Values of $b$, $c$, $\alpha$, and $\gamma$ observed for K-rich feldspars (filled circles) and the K equivalents of albite polymorphs (circles) plotted against $\Delta(bc)$. The solid lines for $\alpha$ and $\gamma$ indicate the limiting envelopes of values for these parameters; the dashed lines are largely fortuitous (see text).

Fig. 4. Values of $b$, $c$, $\alpha$, $\gamma$, and $\Delta 2\theta = 2\theta_{131}$-$2\theta_{1\bar{3}1}$ °CuK$\alpha$ observed for Na feldspar (circles), and the Na-rich equivalents of K-rich feldspars (filled circles) plotted against $\Delta(bc)$.

same total Al in $T_1$. Natural feldspars whose powder diffraction patterns are triclinic such as Spencer (1937) samples E and H have Al contents in $T_1$ sites estimated to be between the values for Spencer samples B and C, whose diffraction patterns are monoclinic. There is no single identifiable point on the plots of cell angles in figure 3 that corresponds to the symmetry change. The data plotted in figure 3 for natural triclinic K feldspars and adularia B seem to characterize a unique series, but this is fortuitous. Note also that the curves in figures 2 and 3 of Colville and Ribbe (1968), used to relate optical properties to structural state, are also fortuitous; they are *not* unique and should not be used in a determinative manner.

The unit-cell angles show a limiting series defined by the data for Na feldspars (solid line in fig. 4) or the K equivalents of Na feldspars (solid line in fig. 3). The asymmetric Al/Si distributions of these feldspars show the greatest obliquity ("triclinicity") possible, and presumably all intermediate values can occur. Therefore, a classification of structural state that depends on axial parameters has a clear superiority over one based in whole or in part on angular parameters for the purposes of correlating the structural states of sodic or potassic feldspars or their alkali-exchanged equivalents, as well as natural intermediate compositions.

There are some problems in interpreting the meaning of the curves for $\alpha$ and $\gamma$ for the Na-exchanged K feldspars. The curves shown are based on the arguments of Wright and Stewart (1968) that these angles for the pure Na equivalents of K feldspars, which are monoclinic by powder diffraction methods, are the same as those of high albite, but it is recognized that the position at which $\alpha$ and $\gamma$ first differ from the angles found in high albite is arbitrary. By single crystal methods the change might occur to the right of the point for Spencer C, because streaking and additional reflections which indicate triclinic domains might become apparent before they could be detected in a powder diffraction pattern.

The variation of total Al in $T_1$ with the $2\theta_{131}$-$2\theta_{1\bar{3}1}$ separation (hereafter called $\Delta 2\theta$) shown in figure 4 is gently curved like the relationship for $\gamma$. Consideration of how changes in cell parameters affect $\Delta 2\theta$ (McKie and McConnell, 1963, p. 586) indicates that approximately three-quarters of the change arises from the variation of cos $\gamma^*$. The $\Delta 2\theta$ is easily measured and has been widely used to characterize the structural state of albite and other plagioclases (J. R. Smith and Yoder, 1956; J. V. Smith, 1956; MacKenzie, 1957). We will describe the quantitative relationship between $\Delta 2\theta$ and Al distribution below.

## STRUCTURAL EXPLANATION FOR POSITION ON THE $\alpha^*$-$\gamma^*$ PLOT

The close relationship of $\Delta 2\theta$ and $\gamma$ (and therefore $\gamma^*$) makes it plausible to seek a quantitative structural explanation for the position of alkali feldspar cell angles on the $\alpha^*$-$\gamma^*$ quadrilateral of MacKenzie and Smith (1955). The quadrilateral was divided into 10 equal portions in a manner similar to the *b-c* plot; values for the corners were determined from published and unpublished data: low albite, $\alpha^* = 86°23.7'$, $\gamma^* = 90°27.8'$; high albite, $\alpha^* = 85°57.4'$, $\gamma^* = 87°59.1'$; maximum microcline, $\alpha^* = 90°24.5'$, $\gamma^* = 92°16.5'$; for all monoclinic feldspars $\alpha^* = \gamma^* = 90°$. The low albite-maximum microcline edge was assigned a value of 1.0, and the high albite-high sanidine edge was assigned 0.0. Relative position thus can be expressed as a fractional quantity, designated $\Delta(\alpha^*\gamma^*)$ after J. V. Smith (1968).

There are only a few data points available for structurally analyzed feldspars. All monoclinic feldspars plot at $\alpha^* = \gamma^* = 90°$; for these specimens $\Delta(\alpha^*\gamma^*) = 0$. For completely disordered high albite, $\Delta(\alpha^*\gamma^*) = 0$, and for low albite and maximum microcline (assuming complete Al/Si order, as before) $\Delta(\alpha^*\gamma^*) = 1.0$. The only other data point is Spencer U and its Na-exchanged equivalent (Wright and Stewart, p. 61, table 2 and fig. 3B). The $\Delta(\alpha^*\gamma^*)$ of both samples is the same within measurement errors (0.33 and 0.30), indicating little change in Al/Si distribution during alkali exchange. As expected, reverse exchange returned the cell parameters to close to their original values [$\Delta(\alpha^*\gamma^*) = 0.31$].

Wright and Stewart (1968, table 2 and fig. 3B) found $\Delta(\alpha^*\gamma^*) = 0.0$ for monoclinic K feldspars and their Na-exchanged equivalents and the same values for $\Delta(\alpha^*\gamma^*)$ for each intermediate structural state of albite and its K-exchanged equivalent.

From consideration of structural data for the plagioclase feldspars Ribbe (1968) has deduced the relationship between $\Delta 2\theta$ or $\gamma^*$ and the Al content of the T sites. His $\Delta$Al parameter can be restated here, with no change in value, to be

$$\Delta \mathrm{Al} = \mathrm{Al}_{\mathrm{T}_1} \; - \mathrm{Al}_{\mathrm{T}_1}$$

Inspection of table 1 shows that $\Delta$Al for Spencer U is 0.36. Assuming complete order, $\Delta$Al = 1.0 for maximum microcline and low albite, and $\Delta$Al = 0.0 for completely disordered high sanidine and high albite. The apparent one-to-one correspondence of relative position on the $\alpha^*$-$\gamma^*$ plot and $\Delta$Al leads us to the assumption that $\Delta(\alpha^*\gamma^*)$ and $\Delta$Al are equivalent. We can thereby express quantitatively J. V. Smith's (1968) suggestion that ". . . . $\Delta(\alpha^*\gamma^*)$ measures the unbalance between (O) and (m) sub-sites." We find it useful in what follows to distinguish carefully between $\Delta(\alpha^*\gamma^*)$, the relative position on the quadrilateral, and $\Delta$Al, the difference in the Al contents of the $T_1$O and $T_1$m sites which previously could only be measured by a crystal structure determination and interpretation of the resulting T-O distances. However, from our choice of coordinates conversion between the two quantities is simple. The relationship between $\Delta(\alpha^*\gamma^*)$ and $\Delta$Al depends only on Al/Si distribution and not on composition.

## ESTIMATES OF Al/Si DISTRIBUTION

The distribution of Al over the sites in alkali feldspar of any structural state can now be estimated. This is done by estimating Al in $T_1$ from $\Delta(bc)$, obtaining Al in $T_2$ by difference, and distributing the Al in $T_1$ from $\Delta(\alpha^*\gamma^*)$, where

$$\mathrm{Al}_{\mathrm{T}_1} = \frac{\mathrm{Al}_{\mathrm{T}_1} + \Delta(\alpha^*\gamma^*)}{2} \text{and } \mathrm{Al}_{\mathrm{T}_1\mathrm{m}} = \mathrm{Al}_{\mathrm{T}_1\mathrm{O}} - \Delta(\alpha^*\gamma^*).$$

The Al in $T_2$ sites can be divided equally between $T_2$O and $T_2$m, because all available feldspar structure analyses show nearly equal T-O bond lengths for these sites.

As an example of this procedure, consider three synthetic albites with intermediate structural states: S62-34 and albite III (Wright and Stewart, 1968, table 2 and fig. 3B) and albite R298 prepared by Waldbaum (ms) by heating Amelia albite at 1060°C for 173 hours. The data for R298 in Waldbaum's thesis are $b = 12.8043$, $c = 7.1423$, $\alpha^* = 86°\, 16.0'$, $\gamma^* = 89°\, 41.4'$. From the *b*-*c* plot, total Al in $T_1$ for these samples is predicted to be 0.63, 0.77, and 0.87; $\Delta(\alpha^*\gamma^*)$ equals 0.25, 0.47, and

0.73.[3] Distributions determined by the procedure given above appear in table 3. These indicate nearly equal Al occupancy for $T_1m$, $T_2O$, and $T_2m$, a feature common to the four low plagioclases of different Si/Al ratios whose structures are known (Smith and Ribbe, in press, fig. 3).

The Al/Si distribution is more easily determined for monoclinic feldspars in which the $T_1$ sites are equivalent to one another, and $\Delta(bc)$ is sufficient to estimate the total Al in $T_1$.

## RELATION OF $\Delta 2\theta$ AND $\Delta$Al IN PLAGIOCLASES, INCLUDING ALBITE

Both $\Delta(\alpha^*\gamma^*)$ and $\Delta 2\theta$ are strongly dependent on $\gamma^*$ (or y), and a plot of one against the other is linear (fig. 5). Thus only $\Delta 2\theta$ of albite need be measured and used with figure 5 to estimate $\Delta(\alpha^*\gamma^*)$ and hence $\Delta$Al. The relationship between $\Delta 2\theta$ and $\Delta$Al (Ribbe, 1968) for plagioclase of composition $An_0$ to $An_{35}$ exactly reproduces the line on figure 5 from $\Delta 2\theta = 1.06$ to 1.75. This simply indicates that Al/Si disorder has the same effect on $\Delta 2\theta$, whether the disorder is caused by redistribution of Al and Si amongst the four T sites of albite (as in the low $\rightleftharpoons$ high albite inversion) or by the redistribution required as CaAl substitutes for NaSi in the plagioclase series.[4] Using the $\Delta 2\theta$-$\Delta$Al relationship from the low plagioclase series, the $\Delta$Al's of the three intermediate albites discussed above are very nearly the same as those obtained from the $\Delta(\alpha^*\gamma^*)$ plot, providing further independent evidence for the validity of the equivalence of $\Delta(\alpha^*\gamma^*)$ and $\Delta$Al.

## THE ORDERING PROCESS IN Na FELDSPAR

In Na feldspar the ordering sequence, though complex, can be partially described. It is possible that a truly monoclinic phase might exist at temperatures near the melting point, but after sufficient cooling has occurred and before ordering begins, the framework collapses about the small Na atom, and triclinic symmetry results. Based on our knowledge of the structure of high albite at room temperature (Ribbe, Megaw and Taylor, in press) and certain bonding considerations (Brown, Gibbs, and Ribbe, in press) it is possible to predict why Al concentrates in $T_1O$ and not in $T_1m$. Both $T_1O$ and $T_1m$ are bonded to $O_A1$ which is bonded to two large cations. Energetically $T_1O$ is favored over $T_1m$ because, once cooling has progressed to the point where high albite is distinctly triclinic, the T-O-T angles at the oxygens bonded to $T_1O$ are on the average smaller than those at the oxygens bonded to $T_1m$ (9° smaller in the high albite structure at room temperature). This indicates less $\pi$-bond character for $T_1O$-O bonds than for $T_1m$-O bonds. The $\pi$-bond character for the Si-O bond is 1.5 to 2.0 times as great as

---

[3] The estimated errors of these values and the individual site occupancies derived from them are difficult to evaluate. There are small errors associated with the corners of the quadrilateral, larger errors associated with the cell parameters of each sample, and unevaluated, possibly systematic, errors associated with our assumption of complete order for the lowest structural states. Our opinion is that the cumulative error is less than 0.07 for Al-rich sites and less than 0.04 for Si-rich sites (see table 3).

[4] Specific details and the effects on the *b* and *c* cell edges that have similar causes will be treated in a forthcoming paper by Ribbe and Stewart.

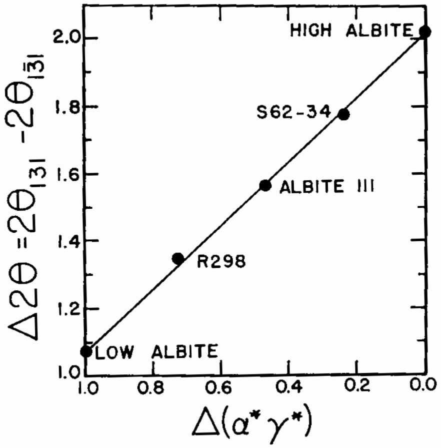

Fig. 5. Plot of $\Delta(\alpha^*\gamma^*)$ against $\Delta 2\theta = 2\theta_{131}\text{-}2\theta_{1\bar{3}1}$ °CuKα.

that for the Al-O bond (Brown, Gibbs, and Ribbe, in press); therefore, Si will prefer $T_1m$ and Al $T_1O$. In addition, the mean of 5 Na-O distances to the oxygens bonded to $T_1O$ is 0.1Å shorter than that to $T_1m$, also indicating that there are less electrons (lower bond order) involved in T-O bonds to $T_1O$ than to $T_1m$. Interestingly, the same angular relationships and Na-O bond considerations occur for the ordered low albite and reedmergnerite structures, so the bond character does not change with T-site occupancy. Predictably, $T_1O$ has a smaller mean T-O-T angle than $T_1m$ in triclinic K feldspars; it also has a shorter mean K-O bond to its four coordinating oxygens than $T_1m$.

Albite polymorphs have been prepared by synthesis from Ab glass, gel, and other compositions and also by heating of lower structural states to yield higher structural states. A great variety of times, temperatures, and pressures were used in these experiments, yet all the data for all albite polymorphs known to us fit the curves in figure 4 closely. The cell parameters of 11 representative structural states of albite synthesized by MacKenzie (1957) were sent to us by W. L. Brown (written commun., 1967). These cell parameters, except *a*, plot as close to the curves in figure 4 as those points shown on the figure, as do the cell parameters of four samples of albite with relatively low structural states supplied to us by R. F. Martin (1967). It appears that, if the $\Delta 2\theta$ (or $b$, $c$, $\alpha$, or $\gamma$) is known, the other cell parameters can be closely estimated from this graph for Na feldspars. The lowest structural state synthesized by MacKenzie (1957) had $\Delta 2\theta = 1.41°$, and the lowest structural state synthesized by Martin had $\Delta 2\theta = 1.176$. The Al distribution in these samples is estimated from figures 4 and 5 and is given in table 3.

The simplicity of the variations observed suggests that only a single ordering process is followed under all circumstances. The ordering process is probably continuous judging from data for annealing experiments like those of MacKenzie (1957). McConnell and McKie (1960) subjected MacKenzie's data to rate analysis and obtained estimates of equilibrium $\Delta 2\theta$ values at various temperatures that plot against temperature as two straight line segments intersecting at about 550° and $\Delta(\alpha^*\gamma^*)$ of 0.33. As ordering proceeds on cooling from the disordered state, the Al contents of $T_1O$ and $T_1m$ first diverge linearly at a low rate. Below about 550°C the rate of divergence of their Al contents increase markedly but again apparently in a linear way. To describe the ordering path in further detail, we need to know the $\Delta(bc)$ values of the intermediate equilibrium states. Because data for albite polymorphs fit the curves shown on figure 4 we have estimated $\Delta(bc)$ from the curve for $\Delta 2\theta$; the estimate is in good agreement with the estimate using $b$ and $c$ directly in those instances where the data are available to us. Utilizing the method of estimating Al distribution described above, we obtain the results shown on figure 6.

TABLE 3

Estimated Al distributions in intermediate albites in atomic percent

| Sample | $\Delta 2\theta$ | $T_1O$ | $T_1m$ | $T_2O$ | $T_2m$ |
|---|---|---|---|---|---|
| S62-34 | 1.778 | $43._5$ | $19._5$ | $18._5$ | $18._5$ |
| Albite III | 1.565 | $62._2$ | $15._2$ | $11._3$ | $11._3$ |
| R 298 | 1.344 | $79._7$ | $6._7$ | $6._8$ | $6._8$ |
| MacKenzie | 1.410 | $75._0$ | $11._0$ | $7._0$ | $7._0$ |
| Martin | 1.176 | $91._8$ | $3._8$ | $2._2$ | $2._2$ |

Several points shown in figure 6 require discussion. Above 550°C the Al contents of $T_1m$, $T_2O$, and $T_2m$ are approximately equal. Below 550°C the Al content of $T_1m$ could possibly be slightly less than either of the $T_2$ sites, although within the limits of error, and from bonding considerations this is not likely. As shown in the figure, the Al content of $T_1m$ does not increase above its initial value, 0.25 for high albite. As $\Delta(bc)$ is insensitive to the distribution of Al between the $T_1$ sites, and $\Delta(\alpha^*\gamma^*)$ only indicates the difference between the Al distributions in the $T_1$ sites, there is a possibility within the limitations of our method that the Al contents of both sites increase, $T_1O$ at a greater rate than $T_1m$.

The ordering scheme described involves simultaneous regular migration of Al from $T_2$ sites and $T_1m$ into the $T_1O$ site. Gentle heat treatment will reverse the process in some samples, but disordering by considerable overheating can drive Al from $T_1O$ sites into all other sites and can result in the presence of two structural states in the heated products at intermediate stages—one only partially disordered and the other nearly completely disordered (Stewart and von Limbach, 1967, p. 395; Smith, J. R., 1956, p. 189).

## THE ORDERING PROCESS IN K FELDSPAR

Whereas disordered albite appears to be triclinic, even at temperatures near its melting point, disordered K feldspar is monoclinic. Laves

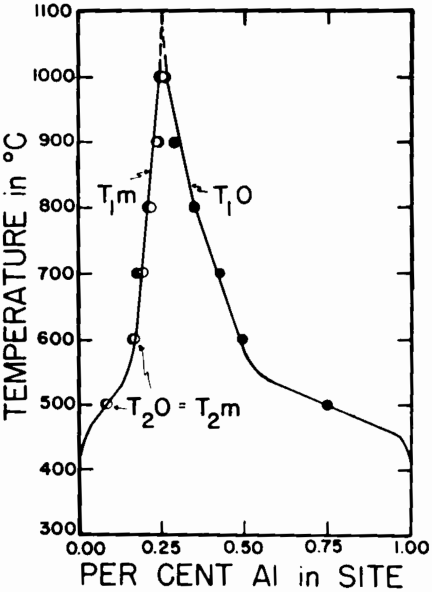

Fig. 6. Al distribution over the four tetrahedral sites in albite as a function of temperature, as deduced by the method described in the text.

and Goldsmith (1961) and Brown (1962) have illustrated and discussed the ordering process in K feldspar in some detail. We remark here that high resolution single crystal X-ray photographs and electron photomicrographs have demonstrated the presence of minute twin-related triclinic domains that result from the random migration of Al into the equivalent $T_1O$ and $T_1m$ sites (Brown, 1962; McConnell, 1965; Colville and Ribbe, 1968), even though X-ray powder diffraction and optical methods average the Al/Si distribution and give the appearance of monoclinic symmetry. Al migrates to the $T_1$ sites because $T_1$ is bonded to $O_A1$ which is in turn the only oxygen bonded to two large metal cations (K, Na, or Ca). Thus, simple electrostatic considerations govern the preference of Al for $T_1$.

Similar bonding arguments apply to both Na and K feldspars; in fact, the ordering path for the two is not conceptually different. The only apparent difference is that K feldspar begins to order with monoclinic restraints, but on the unit-cell scale these rapidly disappear as twin-related triclinic domains nucleate and grow, eventually giving way to topologically distinct, twin-related macroscopic units. Only from the point of view of long-range order which averages Al/Si distribution over thousands of unit cells is the K feldspar ordering path different than the Na feldspar scheme. One process, complicated though it be, is operative in both feldspar end-members; symmetry is a complication for K feldspar, but only rates of ordering, not process, are different. K feldspar orders more slowly than Na feldspar under identical conditions, because twin-related domains formed early in the ordering of K feldspar must be recrystallized into larger neighboring domains to form large macroscopic domains with lower surface energy. Albite, on the other hand, usually goes directly to macroscopic domains which at no stage need be recrystallized to decrease surface energy.

### EFFECT OF RAPID HEATING ON $\Delta(bc)$ AND $\Delta(\alpha^*\gamma^*)$

When sodium feldspar polymorphs are heated so rapidly that neither the total amount of Al in $T_1$ nor its distribution change (Stewart and von Limbach, 1967; Grundy and Brown, 1967) both the $\Delta(bc)$ and $\Delta(\alpha^*\gamma^*)$ plots continue to give accurate estimates of the Al distribution. The angles of maximum microcline do not change on heating (Grundy and Brown, 1967), and the $\alpha^*$ and $\gamma^*$ angles of monoclinic alkali feldspars are not likely to change below the melting point. Thus it appears that our method can be used to estimate the Al distribution over a wide temperature range.

### SUMMARY AND SUGGESTIONS FOR FUTURE RESEARCH

The cell parameters $b$, $c$, $\alpha^*$, and $\gamma^*$ of alkali feldspars may now be used to estimate the Al/Si distribution among the four symmetrically non-equivalent tetrahedral sites of triclinic members and between the two non-equivalent sites of monoclinic members. Relative position on the *b-c* plot gives total Al in $T_1O$ and $T_1m$ or in the two $T_1$ sites; total Al in the $T_2$ sites, where $T_2O = T_2m$, is obtained by difference. Relative position on the $\alpha^*$-$\gamma^*$ plot gives the difference in Al content between $T_1O$ and $T_1m$. Consideration of structural details of the ordering process indicates that alkali feldspar follows a single scheme differing only in symmetry restraints. Specific details for the ordering process in Na feldspars are given in figure 6.

Plots of K feldspar optical parameters, such as 2V and birefringence, "b"-$\alpha$ (Colville and Ribbe, 1968, figs. 2 and 3) are not unique and cannot be used to predict Al/Si distributions or mean T-O bond lengths. It is most convenient and most informative, then, to determine the cell parameters. If 10 mg of material are available, an X-ray powder diffraction pattern is easily obtained and processed by techniques discussed by Wright and Stewart (1968) and Wright (1968), where the *b-c* plot and any one other parameter are used to estimate structural state, composition, and the presence of anomalous dimensions. If available a 0.1 to 0.2 mm single crystal can readily be mounted on (010)–b*, to get $\alpha^*$ and $\gamma^*$ directly from precession photographs and on $a$ to get precise $b$ and $c$ cell edges using a Straumanis-mounted precision back-reflection Weissenberg camera.

We have attempted to utilize available data to suggest methods for estimating the Al distributions of alkali feldspars. The simplifying assumptions of complete order and complete disorder at the extremes of the range of observed structural states appear to be so useful that the attempt to reinvestigate the T-O-Al relationship is welcome (see

Brown, Gibbs, and Ribbe, in press). High precision structural analyses are required to confirm the ordering process described, especially one for an intermediate albite—if necessary, even on a sample carefully heated from the low structural state. Refinements of Spencer E and H should show triclinic distributions in structural states intermediate between those of Spencer samples B and C. The re-refinement of Spencer U to be undertaken by S. W. Bailey (written commun., 1967) should reduce confusion. The contentions of J. V. Smith (1968) regarding the relative importance of local and distant order might be evaluated by high quality X-ray diffraction experiments.

## ACKNOWLEDGMENTS

This paper benefited from discussions with several crystallographers about the common properties of alkali feldspars. Mrs. J. R. Clark performed some early bond length calculations that were especially useful. She, J. V. Smith, D. E. Appleman, G. V. Gibbs, and W. L. Brown have made helpful suggestions and data available and encouraged us to complete this research. P. H. Ribbe was supported in part by National Science Foundation Grant GA-1133.

## REFERENCES

Appleman, D. E., and Clark, J. R., 1965, Crystal structure of reedmergnerite, a boron albite, and its relation to feldspar crystal chemistry: Am. Mineralogist, v. 50, p. 1827-1850.

Bailey, S. W., and Taylor, W. H., 1955, The structure of a triclinic potassium felspar: Acta Cryst., v. 8, p. 621-632.

Brown, B. E., 1962, Aluminum distribution in an igneous maximum microcline and the sanidine microcline series: Norsk geol. tidsskr., v. 42.2, p. 25-36.

Brown, B. E., and Bailey, S. W., 1964, The structure of maximum microcline: Acta Cryst., v. 17, p. 1391-1400.

Brown, G. E., Gibbs, G. V., and Ribbe, P. H., in press, The nature of the Al–O and Si–O bonds in framework silicates: Am. Mineralogist, v. 54, in press.

Clark, J. R., and Papike, J. J., 1967, Silicon-oxygen bonds in chain and framework silicates [abs.]: Am. Cryst. Assoc., Summer Mtg, Minneapolis, Aug. 20-25, p. 91.

Colville, A. A., and Ribbe, P. H., 1968, The crystal structure of an adularia and a refinement of the structure of orthoclase: Am. Mineralogist, v. 53, p. 25-37.

Deer, W. A., Howie, R. A., and Zussman, Jack, 1963, Rock-forming silicates v. 4, Framework Silicates: New York, John Wiley and Sons, 435 p.

Finney, J. J., and Bailey, S. W., 1964, Crystal structure of an authigenic maximum microcline: Zeitschr. Kristallographie, v. 119, p. 413-436.

Grundy, H. D., and Brown, W. L., 1967, Preliminary single-crystal study of the lattice angles of triclinic feldspars at temperatures up to 1200°C: Schweizer min. pet. Mitt., v. 47, p. 21-30.

Jones, J. B., 1968, Al–O and Si–O tetrahedral distances in alumino-silicate framework structures: Acta Cryst., v. B24, p. 355-358.

Laves, F., and Goldsmith, J. R., 1961, Polymorphism, order, disorder, diffusion and confusion in the feldspars: Inst. "Lucas Mallada", Cursillas Conf., v. 8, p. 71-80.

Laves, F., and Hafner, S., 1962, Infrared absorption effects, nuclear magnetic resonance and structure of feldspars: Norsk geol. tidsskr., v. 42.2, p. 57-71.

McConnell, J. D. C., 1965, Electron optical study of effects associated with partial inversion in a silicate phase: Philos. Mag., v. 11, p. 1289-1301.

McConnell, J. D. C., and McKie, Duncan, 1960, The kinetics of the ordering process in triclinic $NaAlSi_3O_8$: Mineralog. Mag., v. 32, 436-454.

MacKenzie, W. S., 1957, The effect of temperature on the symmetry of high-temperature soda-rich feldspars: Am. Jour. Sci., Bowen v., pt. 2, p. 319-342.

MacKenzie, W. S., and Smith, J. V., 1955, The alkali feldspars: I. Orthoclase-microperthites: Am. Mineralogist, v. 40, p. 707-732.

McKie, Duncan, and McConnell, J. D. C., 1963, The kinetics of the low high transformation in albite I. Amelia albite under dry conditions: Mineralog. Mag., v. 33, p. 581-588.

Martin, R. F., 1967, The synthesis of low albite [abs.]: Am. Geophys. Union Trans., v. 48, p. 225-226.

Ribbe, P. H., 1963, A refinement of the crystal structure of sanidinized orthoclase: Acta Cryst., v. 16, p. 426-427.

Ribbe, P. H., 1968, An explanation of the discontinuities at $An_{33}$ and $An_{50}$ in the low plagioclase lattice parameters, $\gamma^*$ and $(2\theta_{131}\text{-}2\theta_{131})$ [abs.]: Geol. Soc. America, Program for Mexico City, p. 247-248.

Ribbe, P. H., and Gibbs, G. V., in press, Statistical analysis and discussion of mean Al/Si–O. bond distances and the aluminum content of tetrahedra in feldspars: Am. Mineralogist, in press.

Ribbe, P. H., Megaw, H. D., and Taylor, W. H., in press, The albite structures: Acta Cryst., v. B24.

Smith, J. R., 1956, Effects of heating natural plagioclases: Carnegie Inst. Washington Year Book 55, p. 188-189.

Smith, J. R., and Yoder, H. S., Jr., 1956, Variations in X-ray powder diffraction patterns of plaglioclase feldspars: Am. Mineralogist, v. 41, p. 632-647.

Smith, J. V., 1956, The powder patterns and lattice parameters of plagioclase feldspars. I. The soda-rich plagioclases: Mineralog. Mag., v. 31, p. 47-68.

———— 1968, Cell dimensions $b^*$, $c^*$, $\alpha^*$, $\gamma^*$ of alkali feldspars permit qualitative estimates of Si, Al ordering: albite ordering process [abs.]: Geol. Soc. America, Program for Mexico City, p. 283.

Smith, J. V., and Bailey, S. W., 1963, Second review of Al–O and Si–O tetrahedral distances: Acta Cryst., v. 16, p. 801-811.

Smith, J. V., and Ribbe, P. H., in press, Atomic movements in plagioclase feldspars: a kinetic interpretation: Contr. Mineralogy Petrology, in press.

Spencer, Edmonson, 1937, The potash-soda feldspars. I. Thermal stability: Mineralog. Mag., v. 24, p. 453-494.

Stewart, D. B., and Ribbe, P. H., 1967, Al/Si ordering, lattice parameters, and composition in alkali feldspars [abs.]: Am. Geophys. Union Trans., v. 48, p. 230.

Stewart, D. B., and von Limbach, Dora, 1967, Thermal expansion of low and high albite: Am. Mineralogist, v. 52, p. 389-413.

Wainwright, J. E. N., and Starkey, John, 1968, Crystal structure of a metamorphic low albite [abs.]: Geol. Soc. America, Program for Mexico City, p. 310.

Waldbaum, D. R., ms 1966, Calorimetric investigation of the alkali feldspars: Ph.D. dissert., Harvard Univ., 247 p.

Wright, T. L., 1968, X-ray and optical study of alkali feldspar: II. An X-ray method for determining the composition and structural state from measurement of $2\theta$ values for three reflections: Am. Mineralogist, v. 53, p. 88-104.

Wright, T. L., and Stewart, D. B., 1968, X-ray and optical study of alkali feldspar I. Determination of composition and structural state from refined unit-cell parameters and 2V: Am. Mineralogist, v. 54, p. 38-87.

———— in preparation, X-ray and optical study of alkali feldspar. III. The nature of distortion in potassium-rich feldspar, nature of intermediate microcline, and possible phase relations of potassium-rich feldspar determined from study of natural suites: Am. Mineralogist.